INSTITUTE OF PHYSICS PUBLISHING METROLOGIA
Metrologia **41** (2004) 407–413 PII: S0026-1394(04)86875-0

Realization of the unit of luminous flux at the HUT using the absolute integrating-sphere method

J Hovila[1], P Toivanen[2] and E Ikonen[1]

[1] Metrology Research Institute, Helsinki University of Technology, PO Box 3000, FI-02015 HUT, Finland
[2] Thermo Electron Oy, PO Box 100, FI-01621 Vantaa, Finland

Received 7 July 2004
Published 5 November 2004
Online at stacks.iop.org/Met/41/407
doi:10.1088/0026-1394/41/6/008

Abstract
A description of a detector-based realization of the unit of luminous flux (lumen) at the Helsinki University of Technology (HUT) is presented. The realization is based on the absolute integrating-sphere method developed at the National Institute of Standards and Technology (NIST), with some modifications. The measurement set-up consists of a 1.65 m integrating sphere, two photometers, a precision aperture and an external luminous-flux source. The characterization and maintenance of the measurement system are described and the uncertainty budget of the realization is presented. The uncertainty analysis indicates a relative expanded uncertainty ($k = 2$) of 4.7×10^{-3} for the realization. According to the results of an earlier bilateral comparison between the HUT and the NIST, the ratio of the measured luminous flux value of HUT to that of NIST was 1.0006 with an expanded uncertainty ($k = 2$) of 10×10^{-3}, including uncertainties due to realization of the units. Another indirect test measurement indicated a corresponding ratio of 0.9984 with the luminous flux measurements of BIPM with an expanded uncertainty ($k = 2$) of 11×10^{-3}, including uncertainties due to realization of the units.

1. Introduction

Luminous flux is a photometric quantity that describes the total optical power of a light source as seen by a human eye. Traditionally absolute luminous flux standard lamps have been calibrated using a goniophotometer [1], where an illuminance standard photometer is precisely moved around the lamp at known distances and the measured illuminance values are added together. This kind of set-up requires a large measurement facility and accurate positioning devices for the photometer. The measurement sequence also takes a long time to complete, which may degrade the accuracy of the measurement due to the drift of the calibrated lamp.

The absolute integrating-sphere method was developed at the National Institute of Standards and Technology (NIST) in 1995 [2–4] and has been previously tested with some modifications at the Helsinki University of Technology (HUT) [5]. In this method, the lamp to be measured is mounted inside a large integrating sphere, and its luminous flux is compared with a known, external luminous flux. The external flux is determined by measuring the illuminance at a precision aperture plane outside the sphere. The known luminous flux is introduced to the sphere through an opening on the sphere wall. The method requires several correction factors, which are obtained by a thorough characterization of the sphere system. The characterization is time-consuming, but afterwards the actual luminous flux measurement is fast and reliable. The characterization of the measurement system includes measurements of the spatial and spectral responsivity of the integrating sphere, spectral differences of the light sources, illuminance non-uniformity at the aperture plane and signal ratio with different angles of incidence on the sphere wall. The spatial responsivity of the HUT sphere coating is measured using a high-intensity white light-emitting diode (LED) [5], whereas the original NIST method used a miniature incandescent lamp.

To the authors' knowledge, only the NIST has reported on the use of the absolute integrating-sphere method for the realization of the lumen, although there has been considerable interest in the method [6, 7]. Thus, an independent confirmation of the feasibility of the method can be considered useful. The HUT luminous-flux unit is successfully realized using the absolute integrating-sphere method, and it is traceable to the unit of illuminance maintained at the HUT [8]. This paper presents detailed descriptions of the characterization and measurement procedures along with updated uncertainty calculations. The performance of the HUT luminous-flux facility and the validity of the uncertainty budget have been verified by conducting international comparisons. Results of these test measurements are presented.

2. The realization

2.1. Principle

'Luminous flux' describes how much visible light a source emits in total over a solid angle of 4π. The amount of lumens that a lamp produces depends on the electric power consumed, the colour temperature and the bulb finish. Typically, a 60 W white incandescent lamp produces about 700 lm.

When a lamp is turned on inside the integrating sphere, the light reflects from the white, diffuse reflective coating numerous times and produces a uniform illuminance on the sphere surface. Since the sphere surrounds the lamp, the illuminance measured at the sphere surface (direct illumination from the lamp excluded) is directly proportional to the luminous flux of the lamp. However, this is only a relative measurement; the absolute level is determined using a known reference luminous flux, Φ_{ext}, which enters the sphere via a port in the wall.

The reference luminous flux is produced with an external light source, and its numerical value is determined by measuring the illuminance at an aperture plane (see figure 1). For an isotropic point source, the calculation of Φ_{ext} is straightforward, since the illuminance, E_v, is given by luminous flux over a known small area A, that is

$$\Phi_{\text{ext}} = E_v A. \tag{1}$$

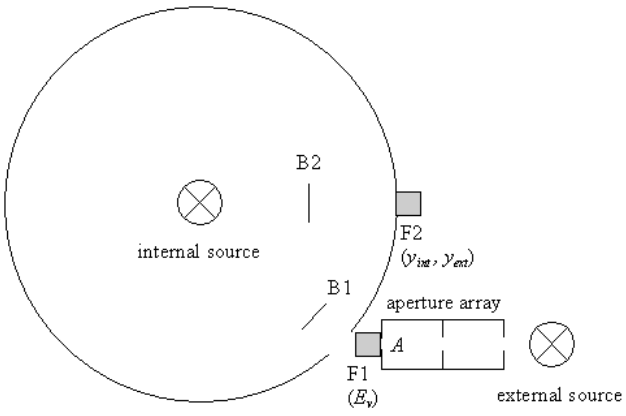

Figure 1. The luminous flux calibration set-up. F1 and F2 are photometers, and B1 and B2 are baffles.

The illuminance standard photometer, which measures the illuminance at the precision aperture plane, provides traceability from the unit of illuminance to the unit of luminous flux.

When entering the sphere, the reference luminous flux produces a signal y_{ext} in another photometer that is attached to the sphere wall. When the external lamp is switched off and the lamp inside the sphere is operated, this sphere photometer produces another signal y_{int}, which is proportional to the measured illuminance. Using the external flux, Φ_{ext}, as the reference source, the luminous flux of the lamp inside the sphere is obtained as

$$\Phi_{\text{int}} = f \frac{y_{\text{int}}}{y_{\text{ext}}} \Phi_{\text{ext}}, \tag{2}$$

where f is a correction factor described below. If all the components of the measurement system were ideal, it would be sufficient to use a correction factor $f = 1$. However, to compensate for some non-ideal features, the numerical value of the correction factor has to be evaluated. The correction factor consists of several components, each of which is a result of a certain characterization measurement. These characterizations include the following:

1. *Spatial correction for the sphere coating*: Integrating spheres have non-uniform surface reflectivity due to uneven thickness and possible contamination of the coating, along with structures such as baffles, the gap between the two hemispheres and a lamp holder. The correction factor for the external flux (incident only on a small part of the sphere wall) needs to be determined.
2. *Spatial correction for the lamp inside the sphere*: The radiation pattern of the lamp inside the sphere affects the uniformity of the illuminance on the sphere wall. Fortunately, as the intensity distributions of the commonly used luminous flux standard lamps are reasonably uniform [9], the spatial correction factor for the internal source can be assumed to be unity, and only its uncertainty needs to be considered.
3. *Spectral mismatch correction for the light sources*: A correction needs to be applied when the spectra of the external and internal light sources are different. Also, the reflectivity of the sphere coating is wavelength-dependent and the sphere photometer probably has a spectral responsivity that differs from the theoretical $V(\lambda)$ curve.
4. *Angle of incidence*: The diffuse reflectance of the sphere coating changes with the incident angle. The external luminous flux hits the sphere wall at a 45° angle, while the light from the internal light source has a normal incidence.
5. *Illuminance non-uniformity at the aperture plane*: The illuminance produced by the external source is measured only at the centre of the precision aperture. However, the illuminance over the aperture area is non-uniform because of the shape of the filament of the external light source. Furthermore, the distance from the external source to the aperture is relatively short and the incoming light has to be considered as a spherical wave with a lower illuminance level towards the edge of the aperture.

2.2. Measurement set-up

The set-up of the luminous flux measurement facility is illustrated schematically in figure 1. It consists of a large integrating sphere, external reference luminous-flux source, internal luminous flux lamp source, illuminance standard photometer F1, sphere photometer F2 and an aperture array with a precision aperture A. Baffles B1 and B2 prevent the light from the internal source from escaping through the opening on the sphere wall or directly illuminating the sphere photometer.

The integrating sphere is manufactured by Labsphere Inc., and it has a diameter of 1.65 m, consisting of two hemispheres with a joint in a vertical plane. The right-side hemisphere in figure 1 is fixed to the floor, while the other part can be moved to allow installation of light sources inside the sphere. The sphere is equipped with a pneumatic opening/closing system. The opening–closing cycle of the sphere has practically no effect on the repeatability of the measurements. The inner surface of the sphere is coated with Spectraflect™, which has an ∼98% reflectance in the visible region.

Inside the sphere a lamp holder is mounted on the top of the right hemisphere about 10 cm from the edge. Therefore, two 45° bends in the supporting rod are needed so that the internal light source is at the centre of the sphere. The lower bend is at a distance of about 55 cm from the lamp socket. The lamp socket has an E27 screw-in base with a four-pole configuration providing separate operating current and base voltage sensing wires. The holder is completely coated with high-reflectance barium sulfate paint. The holder has been designed so that it absorbs the light from the lamp as little as possible. The 180 W Osram Wi40/G Globe operated at 2750 K is a frequently used internal light source.

Both the external light source (1 kW Osram FEL T6) and the internal source are operated by a stable constant-current source. The current of the external lamp is chosen so that the colour temperature is 2856 K. The currents of both lamps are monitored with 100 Ω shunt resistors and digital voltmeters (DVMs).

At a distance of 100 mm from the external light source is an aperture array, which is a light-tight enclosure made of black-anodized aluminium. From the inside, all surfaces are covered with light-absorbing material. The first two openings are for stray light protection, and they are 50 mm in diameter. The last aperture can be chosen from between 30 mm, 40 mm and 50 mm diameter precision apertures; the 40 mm aperture is normally used. The apertures have a shallow, circular embedding for the standard photometer, F1, to ensure proper alignment and distance. Both the external source and the aperture array are mounted on an optical table bolted to the floor.

Both photometers are of type PRC TH15 with temperature-controlled $V(\lambda)$ filters ($f_1' \leqslant 1.5\%$). The illuminance standard photometer has an 8 mm clear aperture, while the sphere photometer has an 8 mm flat diffuser. The photocurrents are passed through a low-noise current-to-voltage converter (CVC). The output voltage of the CVC as well as the lamp currents and base voltages are measured by three DVMs. All measurements are controlled by a computer via a GPIB bus.

2.3. Characterization

2.3.1. Spatial correction. The spatial non-uniformity of the integrating sphere is measured using a spatial scanner placed inside the sphere [5]. The holder of the scanner has the same shape as the lamp holder. The scanner is equipped with two dc minimotors to obtain three-dimensional motion. The sphere surface is scanned using a $5^\circ \times 5^\circ$ scanning grid. To obtain a collimated scanning beam, a white high-intensity LED, together with an achromatic lens, is used as the light source. A stable, low-noise laser diode current driver provides 20 mA dc current for the LED. Relative signals from the sphere photometer are measured for each beam position to obtain the spatial responsivity distribution function (SRDF) $K(\theta, \varphi)$, where θ and φ are the vertical and horizontal angles of the sphere, respectively. The SRDF is normalized to $K^*(\theta, \varphi)$ for the sphere response to an ideal point source, defined as [5]

$$K^*(\theta, \varphi) = \frac{4\pi\ K(\theta, \varphi)}{\sum_{n=1}^{N} \sum_{m=1}^{M} K(\theta_n, \varphi_m) f(\theta_n)\ \Delta\varphi}, \qquad (3)$$

where

$$f(\theta_n) = \begin{cases} \cos(\theta_n) - \cos\left(\theta_n + \dfrac{\Delta\theta}{2}\right), & m = 1, \\ \cos\left(\theta_n - \dfrac{\Delta\theta}{2}\right) - \cos\left(\theta_n + \dfrac{\Delta\theta}{2}\right), & \\ \quad 2 \leqslant m \leqslant (M-1), & \\ \cos\left(\theta_n - \dfrac{\Delta\theta}{2}\right) - \cos(\theta_n), & m = M. \end{cases} \qquad (4)$$

Here $\Delta\varphi$ and $\Delta\theta$ are the intervals of the scanning, and N and M are the number of data points in the vertical and horizontal directions, respectively. The spatial responsivity of the HUT integrating sphere, measured using a white LED, is presented in figure 2. The spatial correction factor for the external source is obtained as

$$k_{\text{ext}} = \frac{1}{K^*(\theta_e, \varphi_e)}, \qquad (5)$$

where (θ_e, φ_e) defines the location of the 'hot spot' (sphere wall location primarily illuminated by the external source).

2.3.2. Spectral mismatch correction. The effect of the sphere coating, i.e. sphere throughput, is defined as

$$T(\lambda) = \frac{E_{\text{in}}(\lambda)}{E_{\text{out}}(\lambda)}, \qquad (6)$$

where $E_{\text{out}}(\lambda)$ is the relative spectral irradiance of a lamp measured with a spectroradiometer outside the sphere, using a photometric bench. After this, the lamp is operated inside the sphere and the relative spectral irradiance $E_{\text{in}}(\lambda)$ of the lamp is measured at the sphere detector port. For this purpose, the sphere photometer F2 is removed and the diffuser-equipped measuring head of the spectroradiometer is placed in the detector port.

The relative spectral response of the system is defined as

$$R_s(\lambda) = R_D(\lambda) T(\lambda), \qquad (7)$$

where $R_D(\lambda)$ is the relative spectral responsivity of the sphere photometer, measured using the HUT spectral responsivity measurement facility [10]. The results show that the relative responsivity is very close to the $V(\lambda)$ curve.

Normalized spectra $S_e(\lambda)$ and $S_i(\lambda)$ of the external and internal light sources, respectively, are measured with a

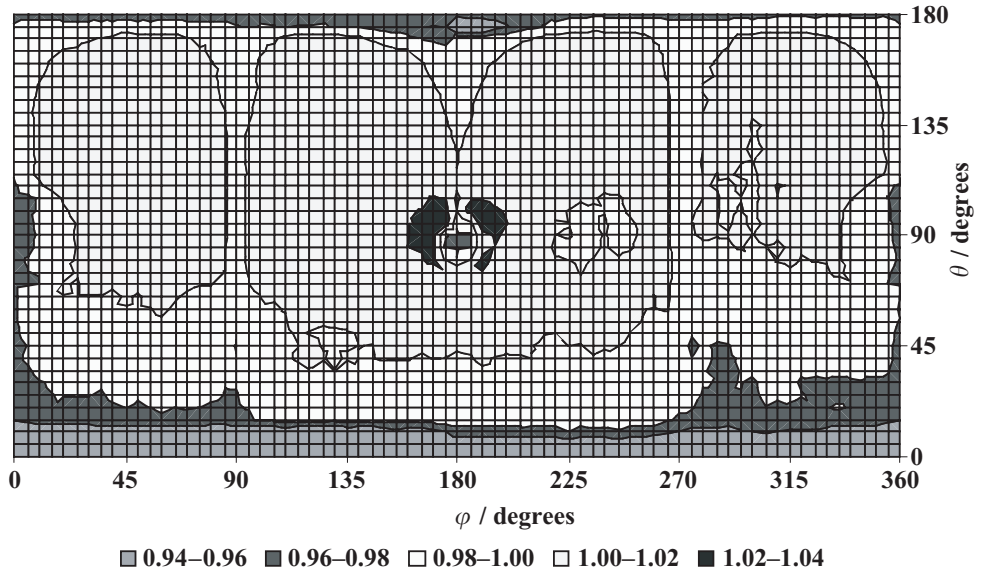

Figure 2. Spatial responsivity of the HUT integrating sphere, measured using a white LED.

spectroradiometer. Using the spectrum of CIE Standard Illuminant A, $S_A(\lambda)$, as the reference, the spectral mismatch correction factor for the internal source can be calculated as

$$c_i = \frac{\sum_\lambda S_A(\lambda) R_s(\lambda) \sum_\lambda S_i(\lambda) V(\lambda)}{\sum_\lambda S_A(\lambda) V(\lambda) \sum_\lambda S_i(\lambda) R_s(\lambda)}. \quad (8)$$

The spectral mismatch correction factor for the external light source, c_e, is calculated by replacing $S_i(\lambda)$ with $S_e(\lambda)$ in equation (8).

2.3.3. Angle of incidence. The incident angle correction factor, β, is measured with the beam light source used for the sphere scanning. While aiming at the hot spot, the beam source is moved from the centre of the sphere to the input axis of the reference luminous flux, keeping the distance to the sphere wall unchanged. The correction factor is obtained as the sphere photometer signal ratio

$$\beta = \frac{S(0^\circ)}{S(45^\circ)}, \quad (9)$$

where $S(0^\circ)$ and $S(45^\circ)$ are the sphere photometer signals for normal and 45° incident angles, respectively. The change in self-absorption due to the different measurement geometry was negligible.

2.3.4. Illuminance non-uniformity of the external source. The illuminance non-uniformity was measured by moving the photometer F1 using an x–y translation stage within the aperture area A. The illuminance non-uniformity correction factor, k_a, was obtained as the average of the measured illuminance values divided by the illuminance at the centre of the aperture.

2.3.5. Combination of correction factors. The results of the characterization measurements can be combined in the correction factor f, which is calculated as

$$f = \frac{k_{int} c_i k_a}{k_{ext} c_e \beta}, \quad (10)$$

Table 1. Correction factors obtained as the results of the characterization measurements. For the value of k_{int}, see section 4.1.

Correction factor	Value
Spatial non-uniformity, external source, k_{ext}	0.9993
Spatial non-uniformity, internal source, k_{int}	1.0000
Colour correction, external source, c_e	1.0003
Colour correction, internal source, c_i	1.0006
Angle of incidence, β	0.9976
Illuminance non-uniformity, k_a	0.9987
Overall f	1.0021

where k_{int} is the spatial correction factor related to the internal source. The numerical values of the correction factors obtained from the characterization measurements are presented in table 1.

2.4. Measurement procedure

The measurement procedure is planned in such a way that the burn time of the luminous flux standard lamps is minimized. The external light source is turned on and the aperture array is closed using a shutter within the front opening. After 30 min, the internal light source is also turned on. When the internal light source has been stabilized for 10 min, the signal y_{int} from the sphere photometer F2 due to the luminous flux of the internal source is measured. The internal source is slowly turned off and the dark current of F2 is measured using two different sensitivities of the CVC (there is a difference of three orders of magnitude between the internal and external luminous flux). The standard photometer F1 is put in its place and its dark current is measured. The aperture array is opened and the illuminance, E_v, at the aperture plane is measured. The photometer F1 is removed, allowing the reference luminous flux to enter the sphere through the opening. The signal y_{ext} from photometer F2 is recorded.

After the initial warm-up period, consecutive luminous flux standard lamps can be measured every 20 min, taking into account the time required for the lamp change.

3. Maintenance of the lumen

The traceability for the unit of luminous flux comes from the unit of illuminance. However, the proven long-term stability of the illuminance unit [8] does not prevent the effects that the changes in the luminous flux measurement system itself might cause. Therefore, to reveal any sudden changes in the performance of any part of the measurement system, the HUT lumen is also maintained by the sphere system characterization and five luminous flux standard lamps of type Osram Wi40/G Globe.

The characterization measurements are conducted on a regular basis. The standard lamps are calibrated once a year to note any changes in the performance of the set-up or drift in one or more lamps. So far, no unexpected significant changes have been discovered. On an average, the luminous flux levels of the five standard lamps have increased 0.37% between 2000 and 2003, and some of this change may be due to a new lamp holder.

4. Uncertainty analysis

The uncertainty components of the realization of the unit of luminous flux are presented in table 2. All known uncertainty components are included, whether significant or not.

4.1. Uncertainty components arising from the characterization and calibration of the measurement system

The uncertainty estimates of the spatial correction factor k_{ext}, the incident angle correction factor β, and the illuminance non-uniformity correction factor k_{a} are based on the standard deviations of repeated measurements ($n = 10$). The difference in results obtained for k_{ext} measured with the white and green LEDs was only 0.0002. The spatial correction factor k_{int} has not been measured, but studies with different lamps having very non-uniform intensity distribution patterns [3, 4] show that the correction factors vary within 0.9995–1.0002. The standard uncertainty arising from this correction for our sphere and Osram Wi40/G Globe lamps can be estimated to be 5×10^{-4} divided by $\sqrt{3}$ for a rectangular probability distribution.

The standard uncertainty of the correlated colour temperature for both light sources is 7.5 K. The standard uncertainty of the ratio of the colour correction factors c_{e} and c_{i} is 2×10^{-4}, derived from the uncertainties arising from the colour temperature and sphere throughput measurements.

The relative standard uncertainty of the unit of illuminance at the HUT is 11×10^{-4} [11]. When the unit is transferred to a secondary standard, the uncertainty is increased by the transfer itself (10×10^{-4}) and the long-term drift of the secondary standard photometer (4×10^{-4}) [8].

The aperture plane of the illuminance standard photometer is not at exactly the same distance from the lamp as the precision aperture. Therefore, a correction is needed for the measured illuminance. The measurement distance from the lamp is 600 mm and the maximum error in the position of the photometer aperture is 0.5 mm. Conversion to standard uncertainty and multiplication by a factor of 2 results in a relative uncertainty component of 10×10^{-4}. The diameter of the precision aperture is measured using a laser interferometer and a moving microscope for edge detection. Usually the 40 mm diameter aperture is used, and the relative standard uncertainty of its area is 3×10^{-4}.

The effect of the stray light on the illuminance standard photometer is measured by blocking the direct radiation inside the aperture array and measuring the photocurrent. It is compared with the signal without blocking. The ratio between these currents is added to the estimated diffraction from the aperture edges, resulting in a relative standard uncertainty component of 1×10^{-4}.

The uncertainty caused by the noise is calculated as the standard deviation of the measured photocurrent. The uncertainties of the current measurements are caused by the uncertainties of the calibration of the CVC using different sensitivities, 1×10^{-4} for a sensitivity of $10^5\,\text{V}\,\text{A}^{-1}$ and 2×10^{-4} for a sensitivity of $10^8\,\text{V}\,\text{A}^{-1}$.

Table 2. Uncertainty budget for the realization of the unit of luminous flux.

Source of uncertainty	$10^4 \times$ relative standard uncertainty	Type of uncertainty
Characterization and calibration of the system		
Spatial correction factor, k_{ext}	5	A
Spatial correction factor, k_{int}	3	B
Ratio of colour correction factors, $c_{\text{e}}/c_{\text{i}}$	2	B
Incident angle correction factor, β	3	A
Illuminance non-uniformity correction factor, k_{a}	3	A
HUT illuminance unit	11	B
Transfer to standard photometer	10	B
Drift of the standard photometer	4	B
Distance of the photometer	10	B
Aperture area	3	B
Stray light	1	B
Drift of the external source	1	A
Noise (illuminance)	3	A
Noise (reference flux)	2	A
Current measurement (illuminance)	1	B
Current measurement (reference flux)	2	B
Measurement of luminous flux		
Non-linearity of the sphere photometer	1	B
Temperature of the sphere	1	B
Noise	1	A
Current measurement	1	B
Other		
Sphere opening/closing	1	A
Repeatability of the measurement (typical)	5	A
Screening due to lamp holder	10	B
Combined standard uncertainty	23	
Expanded uncertainty ($k = 2$)	47	

4.2. Uncertainty of the luminous flux measurement

The linearity of the sphere photometer is essential. The standard uncertainty of the linearity of a single-diode

photodetector at photocurrents under 100 µA is estimated to be 1×10^{-4} [12]. The reflectance of the sphere coating depends on the temperature. The rise in temperature due to a 25 000 lm lamp inside a 2.5 m sphere caused a 3×10^{-4} decrease in measurement signal [3]. The standard uncertainty due to the coating temperature dependence for a 2500 lm lamp inside a 1.65 m sphere is estimated to be 1×10^{-4}. Uncertainty estimates due to noise and current measurement are obtained as in section 4.1.

4.3. Other uncertainty components and expanded uncertainty

The uncertainty arising from the frequent opening and closing of the integrating sphere was studied by repetitive photocurrent measurements in between. The standard deviation of these measurements produced an uncertainty component of 1×10^{-4}. The repeatability of the luminous flux measurements was evaluated by test runs. All the lamps reproduced within 5×10^{-4} relative standard deviation. The new lamp holder has been designed to absorb as little light as possible. It is estimated that the absorption is presently less than half of the difference that was observed between the old and new lamp holders. This leads to a relative standard uncertainty component of 10×10^{-4} due to the remaining absorption.

All the type A uncertainty components are small in table 2. Thus the effective degrees of freedom are close to infinity and the expanded uncertainty for a 95% confidence level can be obtained using a coverage factor of $k = 2$.

5. Test measurements

A bilateral comparison for luminous flux measurements was arranged with the NIST in the summer of 2000. Four NIST luminous flux standard lamps were measured using the HUT measurement set-up, the only difference from the present measurement system being a different lamp holder at the HUT. The comparison showed an excellent agreement between the maintained units [13]. The overall relative difference for four lamps was 6×10^{-4}. The expanded uncertainties ($k = 2$) of the comparison and the agreement of the units were 18×10^{-4} and 101×10^{-4}, respectively.

Another test measurement was conducted in the summer of 2003 with the SP (Swedish National Testing and Research Institute). Two luminous flux standard lamps, previously calibrated by the BIPM in October 2001, were measured at the HUT using the new lamp holder. The results are shown in table 3. The average ratio of the luminous flux values measured by the HUT to those given by the BIPM is 0.9984 with an expanded uncertainty ($k = 2$) of 110×10^{-4}, including uncertainties due to realization of the units.

Table 3. Results of test measurements using the SP lamps traceable to the BIPM. The expanded uncertainty of the BIPM values is 1.0% ($k = 2$).

Standard lamp	HUT (2003)	SP (BIPM, 2001)
246A	2677.3 lm	2679.9 lm
250D	2761.3 lm	2767.3 lm

6. Conclusions

A facility for luminous flux measurements has been constructed at the HUT. The measurement system is based on the absolute integrating-sphere method, which includes a thorough characterization of the measurement system in order to derive correction factors for the measurement result. The performance of the luminous flux measurement facility has been tested by international comparison measurements.

The results of the test measurements can be used to evaluate the relation of the HUT luminous flux measurements to the key comparison reference value (KCRV) of CCPR-K4 [14], if it is assumed that the scale of NIST and the values assigned to the SP lamps have remained unchanged. From the comparison with NIST [11], a ratio of HUT(2000)/KCRV = 0.9985 is obtained for the HUT luminous flux values measured in 2000, and from the data of table 3 a corresponding ratio of HUT(2003)/KCRV = 1.0016 is obtained via BIPM for the HUT measurements in 2003. The apparent 0.31% change of the HUT scale between 2000 and 2003 is in good agreement with the results obtained with the HUT luminous flux lamps, which indicates a potential change of 0.37% due to the new lamp holder.

The absolute integrating-sphere method has several advantages as compared with absolute goniophotometric measurements of luminous flux. The volume of the laboratory space needed by the integrating-sphere set-up is much smaller than that of the corresponding goniophotometric facility. After the characterization measurements, the actual luminous flux measurement with the integrating sphere is fast and reliable. The short burning time (15 min) of the standard lamps increases their lifetime and improves the accuracy of the measurement due to the smaller drift of the lamp. In addition, the self-absorption of the standard lamp is automatically taken into account.

Acknowledgments

The authors thank K Lahti, I Tittonen and E Vahala for their contributions in the early stages of this work. Financial support by the Center for Metrology and Accreditation and the Academy of Finland (grant no 203577) is acknowledged.

References

[1] 1989 *The Measurement of Luminous Flux* CIE Publ. No 84 (Vienna: International Commission on Illumination)
[2] Ohno Y 1996 Realization of NIST 1995 luminous flux scale using the integrating sphere method *J. IES* **25** 13–22
[3] Ohno Y and Zong Y 1999 Detector-based integrating sphere photometry *Proc. 24th Session of the CIE* **1–1** 155–60
[4] Ohno Y 1998 Detector-based luminous-flux calibration using the absolute integrating-sphere method *Metrologia* **35** 473–8
[5] Lahti K, Hovila J, Toivanen P, Vahala E, Tittonen I and Ikonen E 2000 Realisation of the luminous-flux unit using a LED scanner for the absolute integrating sphere method *Metrologia* **37** 595–8
[6] Rastello M L, Miraldi E and Pisoni P 1996 Luminous-flux measurements by an absolute integrating sphere *Appl. Opt.* **35** 4385–91
[7] Ohno Y, Köhler R and Stock M 2000 An ac/dc technique for the absolute integrating-sphere method *Metrologia* **37** 583–6

[8] Toivanen P, Kärhä P, Manoochehri F and Ikonen E 2000 Realization of the unit of luminous intensity at the HUT *Metrologia* **37** 131–40
[9] Ohno Y, Lindemann M and Sauter G 1997 Analysis of integrating sphere errors for lamps having different angular intensity distributions *J. IES* **26** 107–14
[10] Manoochehri F, Kärhä P, Palva L, Toivanen P, Haapalinna A and Ikonen E 1999 Characterisation of optical detectors using high-accuracy instruments *Anal. Chim. Acta* **380** 327–37
[11] Ikonen E and Hovila J 2004 Final Report of CCPR-K3.b.2-2004: Bilateral comparison of illuminance responsivity scales between the KRISS (Korea) and the HUT (Finland) *Metrologia* **41** Tech. Suppl. 02003
[12] Kübarsepp T, Haapalinna A, Kärhä P and Ikonen E 1998 Nonlinearity measurements of silicon photodetectors *Appl. Opt.* **37** 2716–22
[13] Hovila J, Toivanen P, Ikonen E and Ohno Y 2002 International comparison of the illuminance responsivity scales and units of luminous flux maintained at the HUT (Finland) and the NIST (USA) *Metrologia* **39** 219–23
[14] Sauter G, Lindner D and Lindemann M 1999 CCPR Key Comparisons K3a of luminous intensity and K4 of luminous flux with lamps as transfer standards *PTB Report* PTB-Opt-62